Effect of H_2 on the etch profile of InP/InGaAsP alloys in $Cl_2/Ar/H_2$ inductively coupled plasma reactive ion etching chemistries for photonic device fabrication

Sean L. Rommel,[a] Jae-Hyung Jang, Wu Lu, Gabriel Cueva, Ling Zhou,
and Ilesanmi Adesida
*Department of Electrical and Computer Engineering and Micro and Nano Technology Laboratory,
University of Illinois at Urbana–Champaign, Urbana, Illinois 61801*

Gary Pajer, Ralph Whaley, Allen Lepore, Zane Schellanbarger, and Joseph H. Abeles
Sarnoff Corporation, Princeton, New Jersey 08543-5300

(Received 29 January 2002; accepted 22 April 2002)

This study demonstrates etch profile engineering of InP, $In_{1-x}Ga_xAs_{1-y}P_y$, and $In_{0.53}Ga_{0.47}As$ heterostructures results from adding H_2 to standard Cl_2/Ar inductively coupled plasma-reactive ion etching chemistries. Etch rate curves of bulk InP, $In_{1-x}Ga_xAs_{1-y}P_y$, and $In_{0.53}Ga_{0.47}As$ show a general parabolic trend as a function of the H_2 component of the $Cl_2/Ar/H_2$ ratio. Three distinct etching profiles of InP/InGaAsP layers were realized by varying the $Cl_2/Ar/H_2$ ratio. Highly anisotropic profiles result for $Cl_2/Ar/H_2$ ratios between 2/3/1 and 2/3/2. Waveguiding structures fabricated using this technology are presented with a loss as low as 2 dB/cm. An InP racetrack resonator with a quality factor $(Q)>8000$ is also presented.
[DOI: 10.1116/1.1486232]

I. INTRODUCTION

A fundamental building block of planar lightwave integrated circuits, known as a ring resonator, consists of a straight waveguide segment adjacent to a ring waveguide separated by a narrow air gap. An input signal launched into the straight waveguide segment couples into the ring resonator via the air gap if it is narrow enough to allow a wavefunction overlap (i.e., a spacing <300 nm). It is desirable to make the ridge waveguide narrow so that the structure supports only a single transverse mode and the tail of the eigenmode ''leaks out'' of the ridge to ensure coupling to the resonator. This basic structure acts as a notch filter. When the wavelength is on-resonance, the signal ideally propagates only in the ring; when the transmission is off-resonance, the signal is only transmitted through the straight waveguide.

The key to realizing these structures is the development of dry-etching processes that can produce highly anisotropic structures with high edge acuity and smooth surface morphology. Striations on the edge of the waveguides may cause scattering loss, and should be minimized. Recently, such structures have been realized primarily in AlGaAs/GaAs systems.[1–3] InGaAsP microdisk resonators formed by polymer wafer bonding[4] and cascaded InGaAsP/InP resonators have also been demonstrated.[5] However, loss in the structures grown directly on InP substrates has not been studied extensively.

Dry-etching studies of InP have pursued two general chemistries: methane-based etching and Cl_2-based etching. Reactive ion etching studies typically pursued a CH_4/H_2 etch in conjunction with a cyclical O_2 clean to etch highly anisotropic structures.[6] However, this chemistry suffers from a low etch rate of ~60 nm/min, and is undesirable for practical device fabrication. An alternative approach using Cl_2/Ar in a chemically assisted ion-beam etching chamber was established by Youtsey *et al.*[7] In this study, etch rates as high as 2 μm/min were reported for substrate temperatures of 225 °C.

Recently, inductively coupled plasma-reactive ion etching (ICP-RIE) has been used to etch InP.[8–10] Due to its high plasma density, ICP-RIE results in a high ion flux with low ion energies. Thus, ICP-RIE chemistries may be developed that simultaneously maintain high etch rates while minimizing damage from high energy bombardment.

This study presents a $Cl_2/Ar/H_2$ chemistry that was used to etch InP-based waveguides. The composition of $Cl_2/Ar/H_2$ was found to have a strong influence on the degree of undercut in the profile. Under appropriate conditions, a nearly perfect anisotropic profile was achieved. Low-loss characteristics of racetrack resonators etched using the process developed are presented.

II. ETCH RATES AND PROFILES

The samples discussed in this study were etched in a PlasmaTherm SLR 770 ICP-RIE system. Samples were transferred into the etching chamber via a load lock. A rf bias (13.56 MHz) between 0 and 500 W is supplied to the chuck during etching. An inductive coil power (2 MHz) between 0 and 1000 W is supplied to the chamber via a primary coil in the upper electrode. The chamber pressure is maintained by a feedback-controlled throttle valve. Process gases are introduced into the chamber via a series of mass flow controllers calibrated to flow rates as low as 0.1 sccm.

An initial process optimization was performed on InP substrates patterned via a bilayer photoresist mask technology

---

[a] Electronic mail: rommel@uiuc.edu

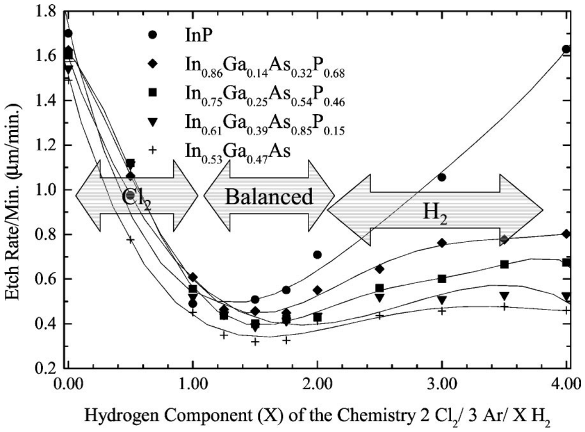

FIG. 1. Etch rate of InP/InGaAsP alloys as a function of the H_2 concentration in ICP-RIE $Cl_2/Ar/H_2$ chemistries. The etch conditions were 900 W inductive power, 110 W rf power, −215 V dc bias, 1.5 mT, 225 °C, and a $Cl_2/Ar/H_2$ ratio of 2/3/*x*. The graph is observed to have three regions: Cl_2 dominated, anisotropic (balanced etch), and H_2 dominated.

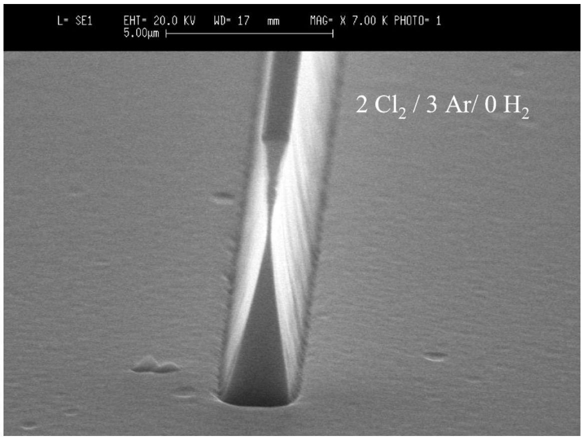

FIG. 2. Scanning electron micrograph of an InP/InGaAsP epitaxial layer etched with 110 W rf power, 900 W inductive power, −215 V dc bias, $Cl_2/Ar/H_2 = 6/9/0$ sccm, 1.5 mT, and 225 °C. These layers exhibit a large undercut of the etch mask, which is still in place.

described elsewhere.[7] Rf power was varied between 50 and 250 W, and the inductive coil power was varied between 300 and 900 W. In accordance with a recent study,[8,9] the chamber pressure was restricted to less than 2 mT to enhance anisotropy. Initially, only Cl_2 was supplied to the chamber. Other than slightly increasing the etch rate, variations to the coil power were found to have little influence on the profile or surface morphology. Therefore, a coil power of 900 W was selected as the optimal operating point, as it resulted in the highest etch rate. In contrast, the profile was strongly influenced by the rf power. An undercut of 0.75 μm was observed for rf powers between 50 and 75 W. As the rf power was increased to 90–120 W, the undercut decreased to 0.45 μm. While etching at higher powers (>150 W) improved anisotropy, the etch mask began to deteriorate, resulting in sidewall erosion of the etched structures. Therefore, despite the undercut, the optimal rf power for a Cl_2 etch was determined to be ~110 W. This undercut was slightly mitigated by the addition of an Ar physical component. A Cl_2/Ar ratio of 2/3 reduced the undercut to 0.25 μm for the present operating conditions. An elevated substrate temperature of 225 °C was introduced to smoothen the etch surfaces, and also to accelerate the etch rate.[7] These conditions (110 W rf power, 900 W coil power, 1.5 mT, Cl_2/Ar ratio of 2/3, substrate temperature of 225 °C) were then fixed to study the role of H_2 on the etch profile. The dc bias resulting from these conditions was −215 V.

A series of five samples with 1-μm-thick epitaxial layers were grown to determine bulk etch rates. The compositions of these layers were InP, $In_{0.86}Ga_{0.14}As_{0.32}P_{0.68}$, $In_{0.75}Ga_{0.25}As_{0.54}P_{0.46}$, $In_{0.61}Ga_{0.39}As_{0.85}P_{0.15}$, and $In_{0.53}Ga_{0.47}As$. The samples were then patterned by contact lithography, and the etch rate was determined by extracting the slope of four etch depth measurements acquired via a stylus profilometer. Figure 1 presents the etch rates obtained for these layers as a function of the H_2 concentration. A fourth-order polynomial was then used to fit the experimental data.

The curves in Fig. 1 can be divided into three regions. In the first region with H_2 ratios between 0 and 1, the etch rates of all of the epitaxial layers decreased with increased H_2 concentration. These data suggest that gaseous H_2 reacts with Cl_2 in the chamber, resulting in a reduction in the number of available radicals responsible for chemical etching. Thus, the etch rate reduces with increased H_2. However, in this region, the amount of Cl_2 exceeded the H_2 and the etch was dominated by Cl_2-chemical etching.

A second region of the graph occurs between H_2 concentrations of 1 and 2. Over this region, the percentages of Cl_2 and H_2 are nearly equal. A slight difference in etch rate is observed as a function of material composition. This region contains the smallest amount of available chemically active species. It is, therefore, believed that in this region etching is dominated by a Cl_2/H_2 chemical etch balanced by an Ar physical component. As data will show later, this region results in the structures with the highest degree of anisotropy.

In the third region of the graph (H_2 concentrations >2), the flow of H_2 begins to dominate the flow of Cl_2. The etching in this region, therefore, is primarily attributed to a H_2 chemical etch. It is observed that the etch rate for all of the epitaxial layers begins to increase above this threshold. However, the degree of increase in the etch rate depends on the material composition. InP clearly shows the highest etch rate whereas $In_{0.53}Ga_{0.47}As$ etches the slowest. The etch rates of the $In_{1-x}Ga_xAs_{1-y}P_y$ quaternary layers increase as the As concentration is decreased. Thus, as the As concentration approaches 0, the layer has an etch rate curve similar to InP, and as the As concentration approaches 100%, the layer has an etch rate curve similar to $In_{0.53}Ga_{0.47}As$. For a $Cl_2/Ar/H_2$ ratio of 2/3/4, it is observed that a selectivity of 4 exists for InP against $In_{0.53}Ga_{0.47}As$.

This information was then used to determine the optimal point for etching device samples. A heterostructure designed for waveguiding was then grown. This layer consisted of

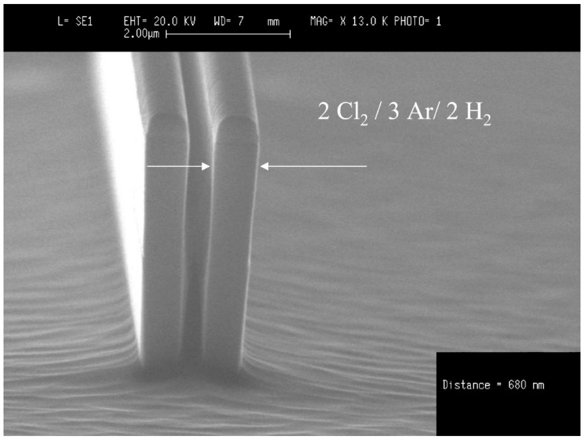

FIG. 3. Scanning electron micrograph of an InP/InGaAsP epitaxial layer etched with 110 W rf power, 900 W inductive power, −215 V dc bias, $Cl_2/Ar/H_2=6/9/6$ sccm, 1.5 mT, and 225 °C. The width of the etched segments is 0.7 μm, and the gap is 0.275 μm. The etch depth is 4 μm.

0.051 μm $In_{0.53}Ga_{0.47}As$, 1.41 μm InP, 0.3 μm $In_{0.86}Ga_{0.14}As_{0.32}P_{0.68}$, 0.09 μm $In_{0.75}Ga_{0.25}As_{0.54}P_{0.46}$, 0.3 μm $In_{0.86}Ga_{0.14}As_{0.32}P_{0.68}$, and 1.5 μm of InP on a semi-insulating InP substrate. A 500-nm-thick SiO_2 mask was deposited on the surface of the sample by plasma-enhanced chemical-vapor deposition. Submicron waveguides were then patterned by electron-beam lithography in a 0.35-μm-thick AZPN114 negative resist. Subsequently, the patterns were transferred to the underlying SiO_2 mask via RIE in a CHF_3 plasma.

This heterostructure was then etched to determine the resulting profile as a function of H_2 concentration. The profile in the Cl_2-dominated region exhibits a large undercut. Figure 2 shows a scanning electron microscope micrograph for the extreme case of $Cl_2/Ar/H_2$ ratios of 2/3/0. As the percentage of H_2 was increased it was observed that the undercut simultaneously decreased. The transition between InP and the InGaAsP layers is not evident in the micrograph, in agreement with the data in Fig. 1. This clearly indicates that the epitaxial layers are etched at approximately the same rates.

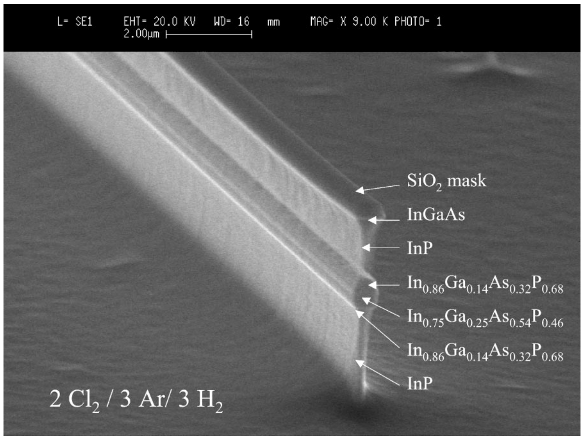

FIG. 4. Scanning electron micrograph of an InP/InGaAsP epitaxial layer etched with 110 W rf power, 900 W inductive power, −215 V dc bias, $Cl_2/Ar/H_2=6/9/9$ sccm, 1.5 mT, and 225 °C. InP layers show large undercuts whereas InGaAsP layers show little lateral etching.

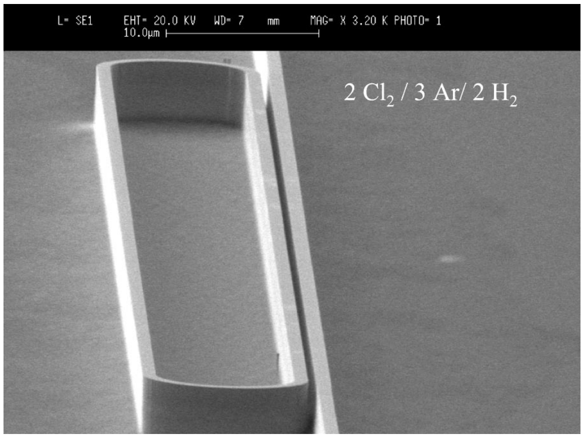

FIG. 5. Scanning electron micrograph of an InP/InGaAsP racetrack resonator fabricated with the process shown in Fig. 3. The ridge is etched to a depth of 5 μm, and has a width of 0.9 μm and gap of 0.275 μm.

Highly anisotropic etching occurs for a $Cl_2/Ar/H_2$ ratio of 2/3/2, in the balanced etching regime. Figure 3 illustrates a section of a racetrack resonator-type structure etched under these conditions. The structure has a linewidth of 0.7 μm, and a gap of 0.275 μm between the line and racetrack. The sidewalls of the structure are very smooth, and show little surface roughness. Note that the gap appears completely etched. Again, it is difficult to discern the positions of the various epitaxial layers in the micrograph, suggesting that the layers have etched at nearly the same rate. Clearly, this chemistry is optimal for fabricating highly anisotropic waveguides.

In the third region (H_2 dominated), the etch profiles show a distinct behavior, which is illustrated in Fig. 4. Once again, InP layers suffer from a 0.15 μm undercut. However, it is evident that the addition of H_2 causes InP and InGaAsP/InGaAs epitaxial layers to etch at different rates. Furthermore, InGaAsP epitaxial layers of varying compositions are observed to etch at different rates as the etch rate data suggested. Three distinct stripes, corresponding to the 0.3 μm $In_{0.543}Ga_{0.457}As_{0.33}P_{0.67}$, 0.09 μm $In_{0.539}Ga_{0.461}As_{0.55}P_{0.45}$, and 0.3 μm $In_{0.543}Ga_{0.457}As_{0.33}P_{0.67}$ waveguiding region are evident in the center of the micrograph. This unique processing condition provides an enabling technology for InP-based nanofabrication. For example, by carefully tailoring the composition of InGaAsP epitaxial layers and the H_2 flow, quantum wires, quantum dots, and cantilever structures may be fabricated.

III. DEVICE FABRICATION AND RESULTS

A series of straight waveguides with widths between 0.7 and 1.0 μm were patterned on the heterostructure layer, and etched with the $Cl_2/Ar/H_2$ ratio fixed at 2/3/2. The samples were etched to a depth of 4 μm to ensure that the waveguiding region was optically isolated from the substrate. The samples were then cleaved to expose an input and output facet. Light was then coupled into the waveguide via a series

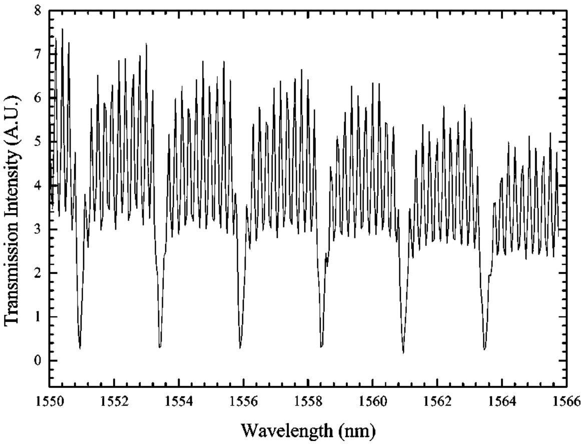

FIG. 6. Resonance data obtained from the device shown in Fig. 5. The quality factor of the device is 8000.

of lenses coupled into a tapered optical fiber. The output signal was coupled into a second fiber. The waveguides were found to have a loss as low as 2 dB/cm.

A racetrack resonator was then fabricated on the same wafer (see Fig. 5). In this design, a straight segment length of 90 μm is used to enhance the coupling between the straight guide and the ring. The ridge width was ~0.9 μm, and the air gap had a width of 0.275 μm. A radius of 15 μm was used in the curved regions. Again, the structure was etched with the optimized $Cl_2/Ar/H_2$ etch to a depth of 4 μm.

Clear resonance data are presented in Fig. 6. Because the ends of the facets were not antireflection coated, Fabry–Pérot resonances are also observed. The structure shows a quality factor of 8000, and a free-spectral range of 2.41 nm. Obtaining a larger free-spectral range can be achieved by reducing the circumference of the racetrack.

IV. CONCLUSION

The positive impact of the addition of H_2 to a Cl_2/Ar process for the etching of InP-based heterostructures was demonstrated. The addition of H_2 balances the physical and chemical components, resulting in three distinct etch profiles. The Cl_2-dominated region ($Cl_2/Ar/H_2$ ratios between 2/3/0 and 2/3/1.5), is typified by high etch rates (1.8 μm/min) and large undercuts of InP and InGaAsP layers. The second region ($Cl_2/Ar/H_2$ ratios between 2/3/1.5 and 2/3/2.5) has balanced chemistry typified by low but uniform etch rates (0.5–0.6 μm/min) and highly anisotropic InP/InGaAsP profiles. A H_2-dominated region occurred for $Cl_2/Ar/H_2$ ratios above 2/3/2.5. In this region, InP layers exhibited large undercuts, whereas InGaAsP layers showed little lateral etching. Experimental evidence also suggests that the selectivity of InGaAsP layers relative to InP may be increased by increasing the As concentration. Waveguides fabricated with a $Cl_2/Ar/H_2$ ratio of 2/3/2 exhibited an insertion loss as low as 2 dB/cm. A racetrack resonator with a quality factor of 8000 was also demonstrated.

ACKNOWLEDGMENTS

The authors wish to thank J. S. Hughes of the University of Illinois at Urbana–Champaign for assistance with the electron-beam lithography. This project was supported by the DARPA/R-FLICs program managed by W. Schneider (DARPA) and monitored by Dr. J. Nichter (United States Air Force Research Laboratory) [Contact No. AF S(490000084) and by NSF-ITR (ANI 01-21662 ITR)].

[1] M. K. Chin, C. Youtsey, W. Zhao, T. Pierson, Z. Ren, S. L. Wu, L. Wang, Y. G. Zhao, and S. T. Ho, IEEE Photonics Technol. Lett. **11**, 1620 (1999).

[2] J. V. Hryniewicz, P. P. Absil, B. E. Little, R. A. Wilson, and P. T. Ho, IEEE Photonics Technol. Lett. **12**, 320 (2000).

[3] P. P. Absil, J. V. Hryniewicz, B. E. Little, R. A. Wilson, and P. T. Ho, IEEE Photonics Technol. Lett. **12**, 398 (2000).

[4] Y. Ma, G. Chang, S. Park, L. Wang, and S. T. Ho, IEEE Photonics Technol. Lett. **12**, 1495 (2000).

[5] Y. Ma, S. H. Chang, S. S. Chang, and S. T. Ho, Electron. Lett. **37**, 564 (2001).

[6] I. Adesida, K. Nummila, E. Andideh, J. Hughes, C. Caneau, R. Bhat, and R. Holmstrom, J. Vac. Sci. Technol. B **8**, 1357 (1990).

[7] C. Youtsey, R. Grundbacher, R. Panepucci, I. Adesida, and C. Caneau, J. Vac. Sci. Technol. B **12**, 3317 (1994).

[8] E. W. Berg and S. W. Pang, J. Vac. Sci. Technol. B **16**, 3359 (1998).

[9] E. W. Berg and S. W. Pang, J. Electrochem. Soc. **146**, 775 (1999).

[10] J. Hong, J. W. Lee, C. R. Abernathy, E. S. Lambers, S. J. Pearton, R. J. Shul, and W. S. Hobson, J. Vac. Sci. Technol. A **16**, 1497 (1998).